THE JOURNAL OF BIOLOGICAL CHEMISTRY VOL. 288, NO. 42, pp. 30614–30625, October 18, 2013

Quantification of Interaction Strengths between Chaperones and Tetratricopeptide Repeat Domain-containing Membrane Proteins*[S]

Received for publication, June 13, 2013, and in revised form, August 14, 2013 Published, JBC Papers in Press, September 13, 2013, DOI 10.1074/jbc.M113.493015

Regina Schweiger[‡], Jürgen Soll[‡], Kirsten Jung[§], Ralf Heermann[§1], and Serena Schwenkert[‡2]

From the Departments of [‡]Biology I, Botany, and [§]Biology I, Microbiology, Munich Center for Integrated Protein Science, Ludwig-Maximilians-Universität München, Grosshaderner Strasse 2–4, D-82152 Planegg-Martinsried, Germany

Background: Tetratricopeptide repeat proteins at organellar surfaces serve as docking proteins for chaperone-bound preproteins.
Results: Binding affinities of docking proteins and chaperones were determined using surface plasmon resonance spectroscopy, Interaction Map® analysis, and microscale thermophoresis.
Conclusion: Docking proteins of the chloroplast, mitochondrion, and endoplasmic reticulum bind differentially to various cytosolic chaperones.
Significance: Tetratricopeptide repeat docking proteins possibly discriminate between chaperones in the cytosol.

The three tetratricopeptide repeat domain-containing docking proteins Toc64, OM64, and AtTPR7 reside in the chloroplast, mitochondrion, and endoplasmic reticulum of *Arabidopsis thaliana*, respectively. They are suggested to act during post-translational protein import by association with chaperone-bound preprotein complexes. Here, we performed a detailed biochemical, biophysical, and computational analysis of the interaction between Toc64, OM64, and AtTPR7 and the five cytosolic chaperones HSP70.1, HSP90.1, HSP90.2, HSP90.3, and HSP90.4. We used surface plasmon resonance spectroscopy in combination with Interaction Map® analysis to distinguish between chaperone oligomerization and docking protein-chaperone interactions and to calculate binding affinities for all tested interactions. Complementary to this, we applied pulldown assays as well as microscale thermophoresis as surface immobilization independent techniques. The data revealed that OM64 prefers HSP70 over HSP90, whereas Toc64 binds all chaperones with comparable affinities. We could further show that AtTPR7 is able to bind HSP90 in addition to HSP70. Moreover, differences between the HSP90 isoforms were detected and revealed a weaker binding for HSP90.1 to AtTPR7 and OM64, showing that slight differences in the amino acid composition or structure of the chaperones influence binding to the tetratricopeptide repeat domain. The combinatory approach of several methods provided a powerful toolkit to determine binding affinities of similar interaction partners in a highly quantitative manner.

Targeting of nuclear-encoded proteins in plant cells requires regulation at several levels to ensure efficient biogenesis and maintenance of organelles. All proteins of the endoplasmic reticulum (ER)[3] as well as almost the entire proteome of chloroplasts and mitochondria rely on being synthesized in the cytosol and transported to and across the correct membranes. All chloroplast and mitochondrial proteins are imported post-translationally, whereas for the endoplasmic reticulum both co-translational and post-translational import has been described (1–3).

All preprotein-translocon complexes are equipped with a central channel protein embedded into the lipid bilayer thus allowing preproteins to travel from the cytosol into the respective organelles. The translocation process through the pore is assisted by associated docking or receptor proteins, which often harbor large cytosolic domains to mediate interaction with preproteins and cytosolic factors. Docking proteins containing tetratricopeptide repeat (TPR) domains are found in almost all organellar membranes and organisms as parts of the translocon complexes (4). Although they do not represent an essential feature for cell viability, causing only mild defects upon deletion, they act as regulators under stress conditions and in concert with other receptor proteins (5–7). The contact between the TPR domains of membrane docking proteins and cytosolic preproteins can either occur directly or indirectly utilizing chaperones bound to the preproteins as scaffold proteins. The C-terminal EEVD motif conserved in cytosolic chaperones such as heat shock proteins HSP70s and HSP90s can be coordinated by the clamp-type TPR domain, which consists of three repetitive

* This work was supported by Deutsche Forschungsgemeinschaft Grant SFB 1035, Project A04 (to J. S. and S. S.), Fonds der Chemischen Industrie Grant Do 187/22 (to R. S.), and the Exc114/1.
[S] This article contains supplemental Fig. 1.
[1] To whom correspondence may be addressed: Munich Center for Integrated Protein Science, Dept. of Biology I, Microbiology, Ludwig-Maximilians-Universität München, Grosshaderner Strasse 2–4, D-82152 Planegg-Martinsried, Germany. Tel.: 49-89-2180-74506; Fax: 49-89-2180-74520; E-mail: heermann@lmu.de.
[2] To whom correspondence may be addressed: Munich Center for Integrated Protein Science, Dept. of Biology I, Botany, Ludwig-Maximilians-Universität München, Grosshaderner Strasse 2–4, D-82152 Planegg-Martinsried, Germany. Tel.: 49-89-2180-74760; Fax: 49-89-2180-74752; E-mail: serena.schwenkert@lmu.de.

[3] The abbreviations used are: ER, endoplasmic reticulum; TPR, tetratricopeptide repeat; HSP, heat shock protein; SPR, surface plasmon resonance; IM, Interaction Map®; MST, microscale thermophoresis; SEC, size exclusion chromatography; Ni-NTA, nickel-nitrilotriacetic acid; Strep, streptavidin.

motifs of 34 degenerate amino acids together forming a helix-turn-helix structure (8).

In mammals and yeast mitochondria, Tom70 is the most prominent TPR domain-containing receptor, which has 11 TPR motifs organized in three distinct domains. The three N-terminal TPR motifs form a clamp-type domain by which it associates with HSP70 in yeast, as well as with HSP90 in mammals. In mammals, Tom70 is assisted by the membrane-associated Tom34, which harbors two TPR domains that interact with HSP70 as well as HSP90, suggesting a possible role as co-chaperone in the cytosol (6, 9–12). Recognized chaperone-preprotein complexes are subsequently released to the Tom translocon, and preproteins are translocated across the outer mitochondrial membrane. Post-translational import into the ER in yeast is also facilitated with the aid of a TPR domain-containing protein, Sec72, that is soluble by itself but anchored to the membrane via Sec71, a membrane-spanning component of the Sec translocon (13). Recently, several post-translationally imported substrate proteins of the secretory pathway have been identified in yeast (3). However, in plants no preproteins of the post-translational translocation pathway into the ER are known to date, which might utilize chaperone guidance. Therefore, it will be interesting to identify candidate proteins in plants in the future and to analyze the role of HSP70 or HSP90 in their delivery to the ER membrane *in vivo*.

In plants, complexity is added to post-translational targeting by the chloroplast as an additional organelle. Likewise, cytosolic components have been described to associate with chloroplast preproteins, such as 14-3-3 proteins as well as HSP70 and HSP90. HSP90-binding candidates are recognized indirectly by the TPR domain-containing protein Toc64 (5, 14–16), a loosely associated component of the chloroplast Toc translocation machinery in the outer envelope membrane. The composition of the Tom complex in plant mitochondria differs distinctively from the complex in yeast and mammals, especially with respect to the receptor proteins. Tom70 is not found in plant genomes; however, a close homologue of Toc64, OM64, has been identified in the outer mitochondrial membrane. Mutants lacking OM64 show reduced import of some mitochondrial proteins, corroborating the idea of a catalytic function of OM64 in protein import dependent on chaperone-assisted translocation (7, 17, 18). Although plants, yeast, and mammals share the central components of the ER Sec translocon Sec61, Sec62, and Sec63, the TPR domain containing Sec72 is only found in yeast. However, we have recently identified AtTPR7 as an interaction partner of *Arabidopsis* Sec63 and Sec62 (19, 20). As we could also show that AtTPR7 can complement the function of Sec72 in yeast and interacts with both HSP70 and HSP90 in pulldown experiments, AtTPR7 is most likely involved in post-translational translocation into the ER in plants. In the plant cytosol, four HSP90 and five HSP70 isoforms exist. Some of these are constitutively produced at high levels, *i.e.* show a minor response to stress exposure (HSP90.2, HSP90.3, HSP90.4, and HSP70.1), whereas other isoforms are heat shock-induced and produced at higher levels under stress conditions (HSP90.1, HSP70.2, HSP70.3, HSP70.4, and HSP70.5) (21, 22).

In this study, we investigated whether Toc64, OM64, and AtTPR7 exhibit preferences for either HSP70 or any of the HSP90 isoforms to investigate a potential supporting function of chaperones in discrimination between organelles during protein sorting. Individual TPR domains of HSP90 co-chaperones have previously been shown to distinguish between HSP70 and HSP90, for example in the HSP70/90-organizing protein, which contains three TPR domains all showing different binding affinities for HSP70 and HSP90 (23). Therefore, we utilized a combination of several biochemical, biophysical, and computational methods to quantify these interactions, including surface plasmon resonance spectroscopy (SPR) with Interaction Map® (IM) evaluation, microscale thermophoresis (MST), as well as *in vitro* pulldown experiments. Interestingly, significant differences were observed with respect to the individual binding affinities of Toc64 and OM64 to HSP70.1 and the HSP90 isoforms. Although the TRP domains are highly similar, OM64 binds preferentially to HSP70.1 and Toc64 binds to both HSP70.1 and the HSP90 isoforms. AtTPR7 binds to HSP70.1 and the HSP90 isoforms in the same manner except for HSP90.1, the heat-induced isoform, for which it shows a reduced binding affinity. Using a combination of SPR and IM analyses, we were able to determine binding kinetics and to quantify these interactions. MST was used as a novel and surface immobilization-independent method to additionally analyze the AtTPR7-chaperone binding affinities.

EXPERIMENTAL PROCEDURES

Cloning and Purification of Recombinant Proteins—Genes encoding the *Arabidopsis* TPR domain-containing docking proteins lacking the transmembrane domain (AtTPR7, amino acids 1–500; Toc64, amino acids 50–604; OM64, amino acids 50–590) were cloned into pET21a$^+$ (Novagen, Darmstadt, Germany), overproduced in *Escherichia coli* (BL21-CodonPlus (DE3)-RIPL) cells, grown in M9ZB medium at 25 °C for 5 h, and purified via nickel-nitrilotriacetic acid (Ni-NTA) affinity chromatography (GE Healthcare, Munich, Germany). HSP90 isoforms were amplified from *Arabidopsis* cDNA using oligonucleotides recognizing the 3′ and 5′ UTR to ensure amplification of the correct isoform. Genes encoding the HSP90 isoforms as well as HSP70.1 were cloned into pET51b (Novagen, Darmstadt, Germany) with an N-terminal StrepII tag. Chaperones were overproduced in *E. coli* (BL21-CodonPlus (DE3)-RIPL) cells, grown in LB medium at 18 °C overnight, and purified via Strep-Tactin affinity chromatography (GE Healthcare). Sequences of all clones were checked by DNA sequencing. Oligonucleotides for AtTPR7, HSP70.1, HSP90.1, HSP90.2, HSP90.3, and HSP90.4 were described previously (19). The following oligonucleotides were used for the OM64 and Toc64 pET21a$^+$ constructs inserting an N-terminal His tag, replacing the transmembrane domain: OM64-NheI-for, 5′-CGATGCTAGCCACCACCACCACCACCACTTAGATCGTTTCGAGCTTC-3′; OM64-XhoI-rev, 5′CGATCTCGAGTCATATGTGTTTTCGGAGTCTC-3′; Toc64-NdeI-for, CGATCATATGCACCCCACCACCACCACCACCCTCCCAAAGCTCCTCATC; and Toc64-XhoI-rev, CGATCTCGAGTCACTGGAATTTTCTCAGTCTC.

Size Exclusion Chromatography—Size exclusion chromatography (SEC) was performed using a Superdex 200 column and

PBS-G buffer (10 mM Na_2HPO_4, 1.8 mM KH_2PO_4, 140 mM NaCl, 2.7 mM KCl, 10% (v/v) glycerin, pH 7.3) as running buffer. 2,000 μM of the receptor protein and 1,000 μM of the respective chaperone were incubated for 1 h at 4 °C and centrifuged at 100,000 × *g* for 15 min before loading on the column.

Time-dependent Ultracentrifugation—Proteins (5 μg in 20 μl) were incubated in PBS buffer (10 mM Na_2HPO_4, 1.8 mM KH_2PO_4, 140 mM NaCl, 2.7 mM KCl, pH 7.3) at 25 °C for 0.5, 1, and 2 h, respectively, and centrifuged at 100,000 × *g* for 15 min, and the supernatant as well as the pellet were subjected to SDS-PAGE. Proteins were visualized by Coomassie Brilliant Blue staining.

SDS-PAGE and Immunoblotting—Proteins were separated on 10% polyacrylamide gels, and immunodetection was performed as described previously (24). HSP90 and HSP70 antisera were generated against wheat chaperones and are described elsewhere (25). Polyclonal Toc64 and OM64 antisera were raised against recombinant *Arabidopsis* proteins (Pineda, Berlin, Germany).

In Vitro Pulldown Experiments—His-tagged TPR proteins (30 μg) were incubated with streptavidin (Strep)-tagged chaperones (500 μM) for 1 h at RT in PBS buffer (140 mM NaCl, 2.7 mM KCl, 10 mM Na_2HPO_4, 1.8 mM KH_2PO_4, pH 7.3). His-tagged proteins were subsequently re-purified by incubation with Ni-NTA for 1 h at RT, and proteins were eluted with 300 mM imidazole in PBS buffer. Proteins were separated on 10% polyacrylamide gels and visualized by Coomassie Brilliant Blue staining.

Surface Plasmon Resonance Spectroscopy—SPR assays were performed in a Biacore T200 (GE Healthcare) using carboxymethyl dextran sensor chips (CM5 Sensor Chip Series S). First, the chips were equilibrated with HBS-EP buffer (10 mM HEPES, pH 7.4, 150 mM NaCl, 3 mM EDTA, 0.005% (v/v) detergent P20) until the dextran matrix was swollen. Then all four flow cells of the CM5 chips were activated by injecting a one-to-one mixture of *N*-ethyl-*N*-(3-dimethylaminopropyl)carbodiimide hydrochloride and *N*-hydroxysuccinimide using the standard amine-coupling protocol. Flow cells 2–4 of each chip were loaded with a final concentration of 10 μg/ml AtTPR7, OM64, and Toc64, respectively, in 10 mM acetate, pH 4.5 (OM64, AtTPR7), or pH 5.5 (Toc64), until surfaces containing densities of 2,000–3,000 resonance units were generated. High immobilization amounts of the receptors were essential to detect binding of the chaperones, putatively due to low "active" receptor concentrations. As running buffer for immobilization of AtTPR7, HBS-EP buffer was used; for immobilization of OM64 and Toc64, PBS-GTM buffer (10 mM Na_2HPO_4, 1.8 mM KH_2PO_4, 140 mM NaCl, 2.7 mM KCl, 10% (v/v) glycerin, 0.05% (v/v) Tween 20, 5 mM β-mercaptoethanol, pH 7.3) was used. Free binding sites of all four flow cells were saturated by injection of 1 M ethanolamine/HCl, pH 8.0. Preparation of chip surfaces was carried out at a flow rate of 10 μl/min. The interaction kinetics of OM64 or Toc64 with the chaperones was performed in PBS-GTM buffer and for AtTPR7 in Strep-binding buffer (50 mM Tris/HCl, pH 8.0, 150 mM NaCl, 1 mM EDTA) at a flow rate of 5 μl/min. Low flow rates emerged best to detect optimal receptor-chaperone binding. The chaperones were diluted in the respective running buffer and passed over all flow cells in different concentrations (0.1–5 μM) using a contact time of 360 s followed by a 300-s dissociation time before the next cycle started. After each cycle, the surface was regenerated by injection of 50 mM NaOH for 30 s at a flow rate of 30 μl/min. All experiments were performed at 25 °C. Sensorgrams were recorded using the Biacore T200 Control software 1.0 and analyzed with the Biacore T200 Evaluation software 1.0. The surface of flow cell 1 was used to obtain blank sensorgrams for subtraction of bulk refractive index background. The referenced sensorgrams were normalized to a base line of 0. Peaks in the sensorgrams at the beginning and the end of the injection emerged from the run time difference between the flow cells of each chip.

Microscale Thermophoresis—MST assays were carried out with a Monolith NT.115 instrument (Nano Temper, Munich, Germany). Purified AtTPR7-His was labeled using the L001 Monolith NT.115 protein labeling kit RED-NHS (Amine Reactive) dye. Increasing concentrations (1 nM to 80 μM) of nonlabeled Strep-tagged chaperones were titrated against 30 nM of labeled AtTPR7-His and centrifuged for 5 min at 16,100 × *g* to remove potential aggregates, and the supernatant was soaked into hydrophilic silicon capillaries (K004 Monolith NT.115). Each measurement was performed three times. Experiments were carried out in 40 mM HEPES, pH 7.5, 20 mM KCl, 0.5 mg/ml BSA, 0.05% (w/v) Tween 20. Data evaluation was performed with the Monolith software.

Interaction Map® Analysis—IM calculations were performed on the Ridgeview Diagnostic Server (Ridgeview Diagnostics, Uppsala, Sweden). For this, the SPR sensorgrams were exported from the Biacore T200 Evaluation Software 1.0 as *.txt files and imported into the TraceDrawer Software 1.5 (Ridgeview Instruments, Uppsala, Sweden). IM files were created using the IM tool within the software, generating files that were sent via E-mail to the server where the IM calculations were performed (23). The result files where then evaluated for spots in the TraceDrawer 1.5 software, and the IM spots were quantified.

Accession Numbers—Sequence data from this article can be found in the NCBI data libraries under accession numbers: At3g17970 (Toc64), At5g09420 (OM64), At5g21990 (AtTPR7), At5g02500 (HSP70.1), At5g52640 (HSP90.1), At5g56030 (HSP90.2), At56010 (HSP90.3), and At5g56000 (HSP90.4).

RESULTS

Toc64, OM64, and AtTPR7 Interact Differentially with HSP70.1 and HSP90 Isoforms—Several TPR domain-containing docking proteins interact with HSP70 and HSP90; however, it is unclear how far they can discriminate between the cytosolic chaperones. For pea Toc64 interaction with the C-terminal peptides of HSP70 and HSP90 was shown, albeit with preference for HSP90 (14). Moreover, HSP90 was shown to be up-regulated in *toc64* mutants, suggesting a more differential function for HSP90 than HSP70 (5). Although OM64 is a close homologue of Toc64, and a parallel function to Tom70 in mitochondria has been suggested, chaperone association has not been investigated to date for this putative chaperone-docking protein. We therefore tested binding of all three *Arabidopsis* TPR domain-containing docking proteins (Toc64, OM64, and AtTPR7) to all cytosolic HSP90 isoforms in *Arabidopsis*,

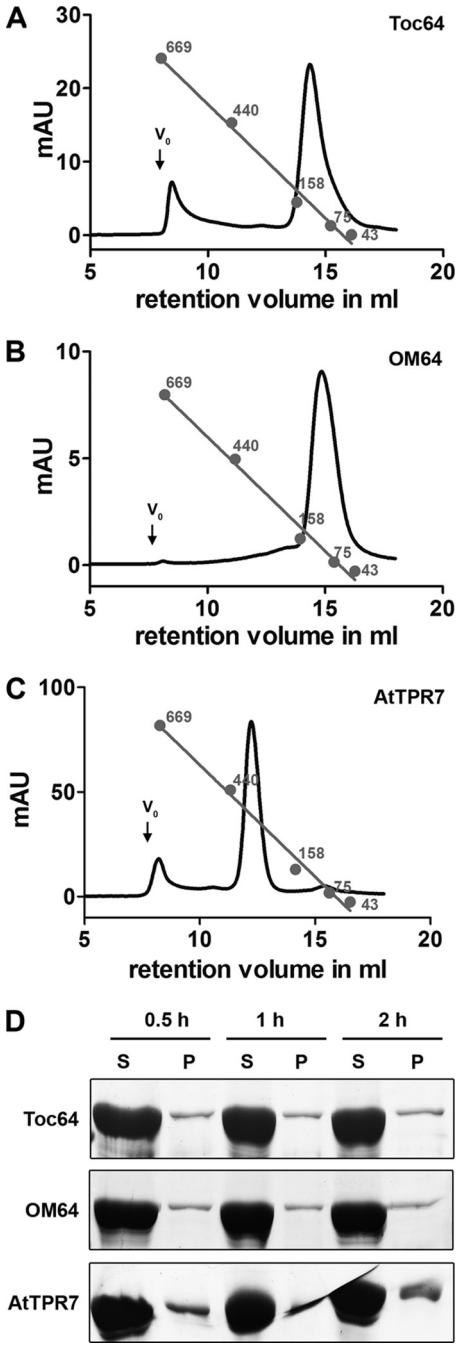

FIGURE 1. **SEC and ultracentrifugation of TPR receptor proteins.** Toc64 (*A*), OM64 (*B*), and AtTPR7 (*C*) were analyzed on a Superdex 200 column. The void volume (V_0) and a calibration curve are indicated. *mAU,* milli-absorption units. *D,* Toc64, OM64, and AtTPR7 were incubated at RT for the indicated time points and subsequently ultracentrifuged. Supernatant (*S*) and pellet (*P*) were analyzed by SDS-PAGE and Coomassie staining.

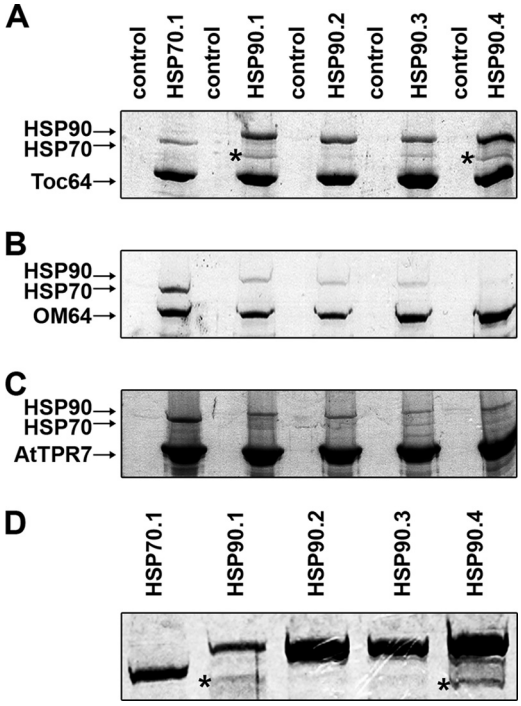

FIGURE 2. **Interaction of chaperone isoforms with TPR receptor proteins.** Recombinant His-Toc64 (*A*), His-OM64 (*B*), and AtTPR7-His (*C*) (30 μg) were incubated with Strep-tagged HSP70.1 and all four cytosolic HSP90 isoforms (500 μM). His-tagged TPR receptor proteins were affinity- purified with Ni-NTA subsequently. All proteins were visualized by Coomassie staining. Samples without His-tagged TPR receptor proteins were used as controls. *D,* purified chaperones as used in the pulldown experiments are shown. Impurities are indicated with *asterisks* and correspond to the likewise indicated bands in *A*.

because HSP90 might act as a supportive factor in the cytosolic protein sorting process. In addition, we tested binding to HSP70.1, because this represents the isoform with the highest basal expression level in *Arabidopsis*. Only one isoform of HSP70 was chosen as HSP70 is known to interact with hydrophobic stretches of almost all preproteins in a rather unspecific manner, and previous analyses did not indicate that the strongly heat shock-induced isoforms are involved in specification of targeting (26).

As a first step, we generated recombinant proteins. For this, the coding sequence of Toc64 and OM64 lacking the N-terminal transmembrane domain and AtTPR7 lacking the C-terminal transmembrane domain were fused to a His tag replacing the transmembrane domain. The recombinant proteins were overproduced in *E. coli* and purified via Ni-NTA. HSP70.1 and HSP90 isoforms were fused to an N-terminal Strep tag, which does not interfere with binding of the C-terminal EEVD motif to the TPR domain, and it was purified accordingly. Because TPR proteins are prone to aggregation in solution, we employed SEC to analyze the status of the purified TPR domain-containing docking proteins (Fig. 1, *A*–*C*). Toc64 and OM64 eluted as monomers, whereas AtTPR7 seemed to form tetramers. Moreover, time-dependent ultracentrifugation was performed (Fig. 1*D*). These analyses also verified that protein aggregation did not occur, even after 2 h of incubation at RT.

Next, we employed an *in vitro* binding assay with the recombinant proteins. His-tagged TPR proteins were incubated either with Strep-HSP70.1, Strep-HSP90.1, Strep-HSP90.2, Strep-HSP90.3 or Strep-HSP90.4 and recovered by Ni-NTA. A sample without His-tagged TPR protein served as a control for each chaperone. The associated chaperones as well as the TPR proteins were separated by SDS-PAGE and detected by Coomassie staining (Fig. 2). Indeed, in accordance with earlier results, more HSP90 than HSP70 was recovered along with Toc64 (Fig. 2*A*). Interestingly, although the protein region of the TPR domain of mitochondrial OM64 displays 68% identity to Toc64, it clearly showed only a weak binding to all HSP90

isoforms, while binding strongly to HSP70.1 (Fig. 2*B*). Similar to our earlier results, AtTPR7 bound to both HSP70.1 and HSP90 isoforms, although binding to HSP70.1 was more prominent (Fig. 2*C*). Note that in this assay no stoichiometric binding behavior can be visualized, because it is not to be expected that each TPR protein bound to nickel beads interacts with a chaperone. Consequently, more TPR proteins than chaperones are visible in all cases. As a control, the recombinant chaperones showing the purity status are presented in Fig. 2*D*.

TPR Docking Proteins Interact with Oligomeric States of Chaperones—Because HSP70 and HSP90 are known to oligomerize (27–30), it was our aim to verify the oligomeric states of the HSP70 and HSP90 proteins used in this work and to analyze their binding to the TPR proteins. SEC was used to separate oligomeric chaperone states as well as receptor-chaperone complexes. Peak fractions were subjected to SDS-PAGE and immunoblot analysis. Two representative interactions were chosen as follows: HSP70.1 with OM64 and HSP90.3 with Toc64. HSP70.1 (71 kDa) without a binding partner was found to oligomerize (Fig. 3*A*), whereas unbound OM64 (62 kDa) eluted as a monomer (Fig. 3*B*). However, upon incubation of HSP70.1 and OM64, a new peak at the size of ~200 kDa appeared (Fig. 3*C*). This peak contained HSP70.1 as well as OM64 (Fig. 3*C*). HSP90.3 (80 kDa) was present as monomers, dimers, tetramers, and oligomers (Fig. 3*D*), whereas Toc64 (59 kDa) also eluted as a monomer (Fig. 3*E*). Upon incubation of Toc64 with HSP90.3, the elution pattern changed, and in addition to HSP90.3 oligomers and Toc64 monomers, a shoulder appeared at ~400 kDa, which contained HSP90.3 and Toc64 (Fig. 3*F*). The chromatograms indicate an interaction of the TPR proteins with chaperone oligomers; however, we could not determine which exact oligomeric state of chaperones and TPR proteins interacts with each other. As HSP70 and HSP90 formed large oligomers, we performed time-dependent ultracentrifugation to ensure that the chaperones are not aggregating. Indeed, after SDS-PAGE and Coomassie staining, almost all protein was found in the supernatant (Fig. 3*D*).

However, no reliable quantitative conclusion could be drawn from the data described above. In the following, we therefore applied further biophysical techniques to analyze the individual binding affinities in more detail.

Determination of Receptor-Chaperone Binding Kinetics by SPR and IM Evaluation—To determine binding kinetics of Toc64, OM64, and AtTPR7 with HSP70.1 and HSP90 isoforms, we performed SPR analyses. For this, Toc64, OM64, and AtTPR7 were immobilized via amino coupling onto a CM5 Sensor Chip, and increasing concentrations (0.1–5 μM) of the chaperones were injected onto the chip surfaces (see "Experimental Procedures" for detail). In all cases, clear binding of the chaperones to the respective sensor surface could be observed (Figs. 4-6*A*). In each experiment, HSP70.1 seemed to bind more strongly to the respective ligand than the HSP90 isoforms. The HSP90.2, HSP90.3, and HSP90.4 isoforms seemed to interact with each receptor with similar affinity. HSP90.1 interaction with AtTPR7 and OM64 was slightly weaker than the other HSP90 isoforms (Figs. 4 and 5*A*). However, none of the sensorgrams followed a final and linear saturation, indicating that the curves did not reflect a single binding event and therefore no clear one-to-one interaction.

As HSP90 and HSP70 oligomerize, it can be assumed that the sensorgrams measured with SPR are a sum of different binding events. On the one hand we observed an interaction of the receptors with the chaperones and on the other hand an interaction of defined oligomeric chaperone states with each other. The even and steady slope of the binding curves indicates a homogeneous interaction of the oligomeric chaperone states. To calculate reliable binding constants and kinetic parameters, a computational approach was chosen to analyze the sensorgrams. The measured curves can be approximated to the sum of primitive binding curves, each representing a monovalent interaction (31) with a unique combination of association rate k_a (on-rate) and dissociation rate k_d (off-rate) (and consequently an equilibrium dissociation constant $K_D = k_d/k_a$). We calculated IMs of each single sensorgram to determine and quantify the individual binding events represented by the curves. The algorithm splits the experimental SPR data set to several theoretical monovalent binding curves and spots the binding curves that, summed up, best fit the experimental data. By plotting the association rate k_a and the dissociation rate k_d within a two-dimensional distribution, it is possible to display heterogeneous binding data as a map where each peak corresponds to one component that contributes to the cumulative binding curve (32). In case that these interaction events have almost similar on- and off-rates, no separate but fused peaks will appear. We interpreted a single peak that extends the size of 1 log magnitude to be composed of two peaks, as theoretically a single interaction event should not vary in binding kinetics by a factor of more than 10. In the IMs presented here, the large peaks that exceed a magnitude of >1 in the log scale were evaluated as fused peaks that are overlapping in a wider area. These peaks were manually split up into two areas and are regarded as two connected individual interactions. The shape of the SPR sensorgrams and the fact that HSP70 as well as HSP90 form oligomers show that the sensorgrams are composed of at least two interaction events. Such a fused peak was most dominant in the AtTPR7-HSP70.1 IM (Fig. 6*B*). Therefore, it was plausible to split those peaks into two peaks with different affinities. As with any evaluation algorithm, there can be a "noise level" in IMs where a peak might be an artifact, either algorithm-related or instrument/data-related. The "fast on/fast off peaks," with a high k_a and a low k_d value, visible in nearly every IM were interpreted to represent bulk effects on the sensor surface. The determination of the peak weight parameter was helpful in this case. Peaks with a weight of less than 4% do not represent real binding events and should therefore be disqualified from data interpretation, whereas those of more than 10% cannot be neglected.[4] In most of the IMs presented in this study, small peaks with high on- and fast off-rates could be observed. These peaks were interpreted as bulk effects and were therefore neglected as they all showed peak weights between 0.1 and 2.0%. In IMs of OM64-HSP70.1, OM64-HSP90.2, OM64-HSP90.3, OM64-HSP90.4, Toc64-HSP70.1, and Toc64-HSP90.4 peaks with a slow

[4] K. Andersson, personal communication.

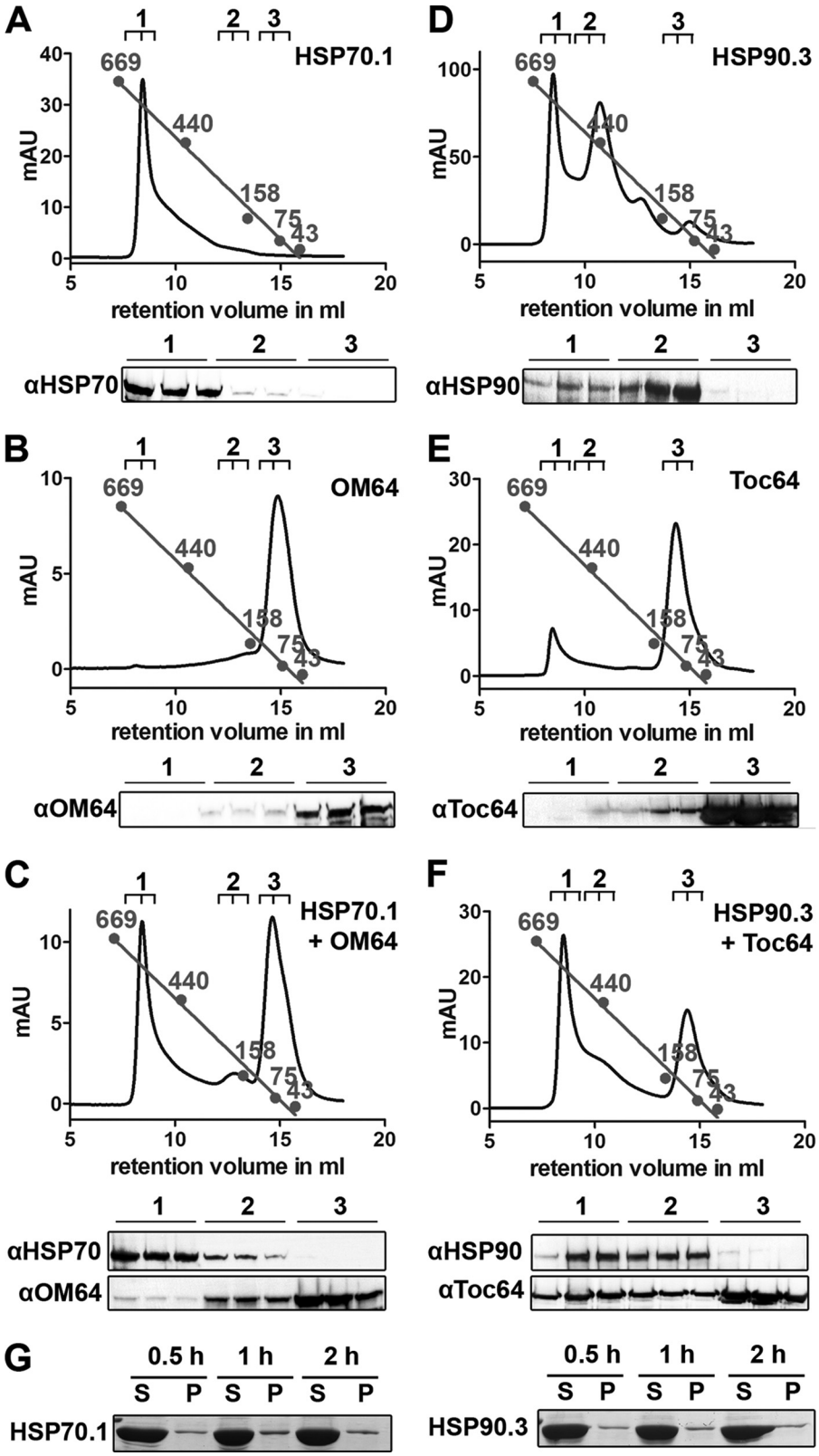

FIGURE 3. **Oligomerization of chaperones and complex formation analyzed by SEC.** HSP70.1 (*A*) and OM64 (*B*) were analyzed individually and after incubation for 1 h at 4 °C (*C*) by SEC. Peak fractions (*1–3*) were analyzed by SDS-PAGE and immunoblotting with the indicated antisera. HSP90.3 (*D*) and Toc64 (*E*) were analyzed individually and after incubation for 1 h at 4 °C (*F*) by SEC. In the case of HSP90.3 (*D*), peaks corresponding to the sizes of monomers, dimers, tetramers, and oligomers are visible. Peak fractions (*1–3*) were analyzed by SDS-PAGE and immunoblotting with the indicated antisera. *G,* HSP70.1 (*left panel*) and HSP90.3 (*right panel*) were incubated at RT for the indicated time points and subsequently ultracentrifuged. Supernatant (*S*) and pellet (*P*) were analyzed by SDS-PAGE and Coomassie staining. *mAU,* milli-absorption units.

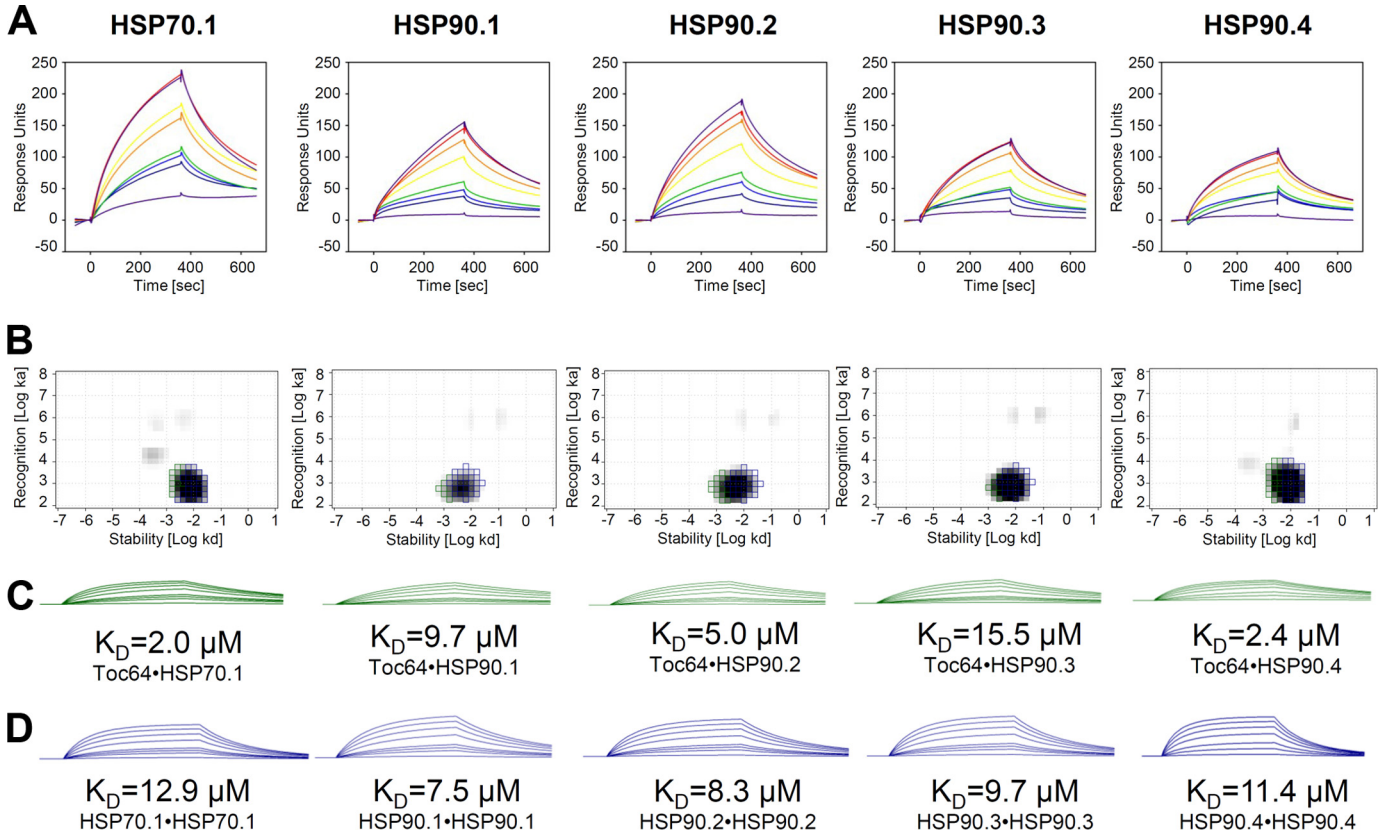

FIGURE 4. **Chaperone binding to Toc64 and determination of binding affinities using SPR and IM analyses.** *A,* SPR analyses. Toc64 was immobilized via amine coupling onto a CM5 senor chip, and solutions of 0.1 μM (*purple*), 0.5 μM (*dark blue*), 0.75 μM (*blue*), 1 μM (*green*), 2 μM (*yellow*), 3 μM (*orange*), 4 μM (*red*), and 5 μM (*dark purple*), respectively, of each of the chaperones were passed over the chip. *B,* IM analyses. The *green spots* represent the Toc64-chaperone interactions and the *blue spots* the chaperone-chaperone interactions (oligomerization). *C,* calculated sensorgrams for Toc64-chaperone interaction. *D,* calculated sensorgrams for chaperone-chaperone interaction. The calculated K_D values for each interaction are indicated *below* the respective sensorgrams.

off-component appeared (Figs. 4–6*B*). These could either result from instrument drift or sticky impurities or represent real binding events. We used the peak weight as cutoff for interpreting these peaks, and we also consulted the results of the pulldown and MST analyses for data interpretation. As the weights of these peaks within OM64-HSP90 isoforms as well as the Toc64-HSP70.1 and Toc64-HSP90.4 IMs were all in the range of 1 and 4%, we neglected these peaks from interpretation. Only the slow off-peak in the OM64-HSP70.1 IM was interpreted as a real binding event, as the peak weight was ~13%.

The calculated interactions are displayed in a peak diagram related to the log of the respective association and dissociation constants, k_a and k_d. The IMs of the chaperones to the respective docking proteins Toc64, OM64, and AtTPR7 are shown in Figs. 4- 6*B*. The calculated sensorgrams for each of the two interaction events that can be extracted from the respective IM analyses are presented in Figs. 4–6, *C* and *D*. We found that in each IM one interaction had similar on- and off-rates. We assumed that the oligomerization of the chaperones should be independent of the presence of the receptor and therefore interpreted the calculated curves in Figs. 4–6*D* (*blue peaks* and *sensorgrams*) to represent the chaperone oligomerization. The K_D values for chaperone-chaperone interaction were calculated to be ~4–13 μM for each of the chaperones in all tested interactions. The calculated sensorgrams with the higher variability in K_D values were therefore assumed to represent the binding events between the different chaperones and the Toc64, OM64, and AtTPR7 receptors, respectively. Toc64 showed binding with similar affinities to HSP70.1 (K_D = 2.0 μM) as to all HSP90 isoforms (K_D = 2.4–15.5 μM) (Fig. 4). In contrast, a very strong interaction could be observed between OM64 and HSP70.1, which showed a K_D = of 0.03 μM (Fig. 5). The HSP90 isoforms interacted with OM64 with much lower affinities compared with HSP70.1. HSP90.2, HSP90.3, and HSP90.4 had a similar affinity to OM64 (K_D = 1.3–2.9 μM) and sole interaction with HSP90.1 was still weaker (K_D = 20.2 μM). For AtTPR7, again HSP70.1 showed the highest affinity (K_D = 1.0 μM) (Fig. 6). The HSP90 isoforms showed comparatively lower affinities (K_D = 5.1–16.0 μM) to AtTPR7. Compared with HSP90.2–4, HSP90.1 binding to AtTPR7 was weaker (K_D = 16.0 μM).

With respect to the binding kinetics, the differences in the receptor-HSP70.1 affinities to the receptor-HSP90s interactions are predominantly caused by differences in the off-rates (k_d) rather than on-rates (k_a) (Table 1). The lowest off-rates were observed for the AtTPR7-HSP70.1 and OM64-HSP70.1 interactions, calculated with $k_d = 5.25 \times 10^{-4}$/s and 3.49×10^{-4}/s, respectively. Only the OM64-HSP70.1 interaction was characterized by a high on-rate ($k_a = 1.25 \times 10^4$/M·s) compared with the other interactions, whereas the AtTPR7-HSP70.1 and Toc64-HSP70.1 on-rates were in a similar range ($k_a = 5.41 \times 10^2$/M·s and 1.55×10^3/M·s). The high affinity of the OM64-HSP70.1 interaction was therefore caused by a high on-rate

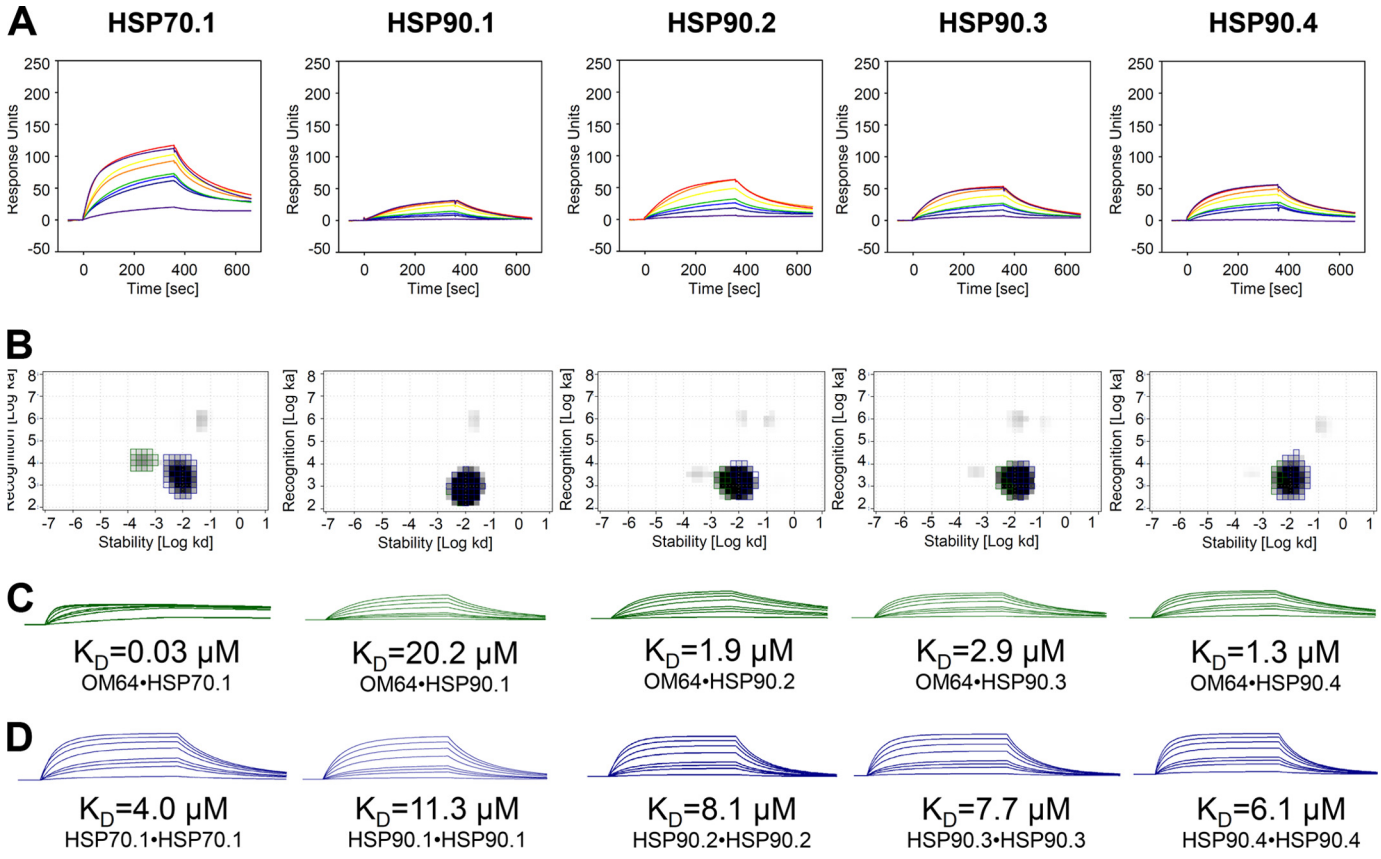

FIGURE 5. **Chaperone binding to OM64 and determination of binding affinities using SPR and IM analyses.** *A,* SPR analyses. OM64 was immobilized via amine coupling onto a CM5 sensor chip, and solutions of 0.1 μM (*purple*), 0.5 μM (*dark blue*), 0.75 μM (*blue*), 1 μM (*green*), 2 μM (*yellow*), 3 μM (*orange*), 4 μM (*red*), and 5 μM (*dark purple*), respectively, of each of the chaperones were passed over the chip. *B,* IM analyses. The *green spots* represent the OM64-chaperone interactions and the *blue spots* the chaperone-chaperone interactions (oligomerization). *C,* calculated sensorgrams for OM64-chaperone interaction. *D,* calculated sensorgrams for chaperone-chaperone interaction. The calculated K_D values for each interaction are indicated below the respective sensorgrams.

($k_a = 1.25 \times 10^4$/M·s), which is almost 10–20-fold higher compared with the Toc64-HSP70.1 (1.55×10^3/M·s) and AtTPR7-HSP70.1 interactions (5.41×10^2/M·s), respectively. The lower affinity of the HSP90.1 isoform compared with the other HSP90 isoforms toward OM64 and AtTPR7 was also mainly caused by lower on-rates rather than higher off-rates. In principle, the off-rates of all other HSP90-receptor interactions were in a more or less similar range and varied around $1–9 \times 10^{-3}$/s.

Determination of Receptor-Chaperone Binding Affinities Using MST Analysis—In contrast to SPR, MST is a novel method to directly monitor protein-protein interaction in solution and is therefore surface immobilization independent. Movement of proteins is monitored in a temperature gradient, and upon binding of the interaction partner, the movement behavior is altered. A fluorescent tag is coupled to one of the binding partners, which allows detection of the thermophoretic movement in a small glass capillary. Upon addition of increasing concentrations of the binding partner, small changes of the hydration shell due to complex formation can be monitored. Binding curves result from changes in fluorescence response (33). To further evaluate AtTPR7-chaperone binding with an additional assay, we employed MST as a second method (Fig. 7). AtTPR7 was coupled to the fluorescent tag, and increasing amounts of chaperones were used as analytes. Weakest binding was again observed for HSP90.1 ($K_D = 2.7$ μM) to AtTPR7. In contrast, constitutively produced HSP90 isoforms showed stronger binding to AtTPR7 with a more than 2-fold lower K_D value (HSP90.2, $K_D = 1.2$ μM; HSP90.3, $K_D = 1.2$ μM; HSP90.4, $K_D = 1.0$ μM). Nevertheless, the strongest binding was monitored for HSP70.1 ($K_D = 0.3$ μM) (Table 2). A similar tendency of the K_D values was observed using both methods. These data go hand in hand with the obtained SPR data, and they also verified the IM calculations from the SPR sensorgrams.

DISCUSSION

The aim of our study was to compare binding affinities of three TPR domain-containing docking proteins, Toc64 at the outer envelope of chloroplasts, OM64 at the outer membrane of mitochondria, and AtTPR7 at the ER membrane, with the cytosolic chaperones HSP70.1 and the four isoforms of HSP90. Members of the HSP70 and HSP90 family have a suggested function in post-translational protein import into the respective compartments. In this context, we aimed to investigate a potential role of HSP70 or HSP90 in the sorting process of preproteins to distinct organelles, because TPR domains of various proteins (*e.g.* HSP70/90-organizing protein) have previously been shown to selectively discriminate between the two chaperones (23, 34, 35). As a first step, we performed *in vitro* pull-down experiments that showed the binding potential of the three TPR domain-containing docking proteins to all tested chaperones, albeit with different intensities. However, because

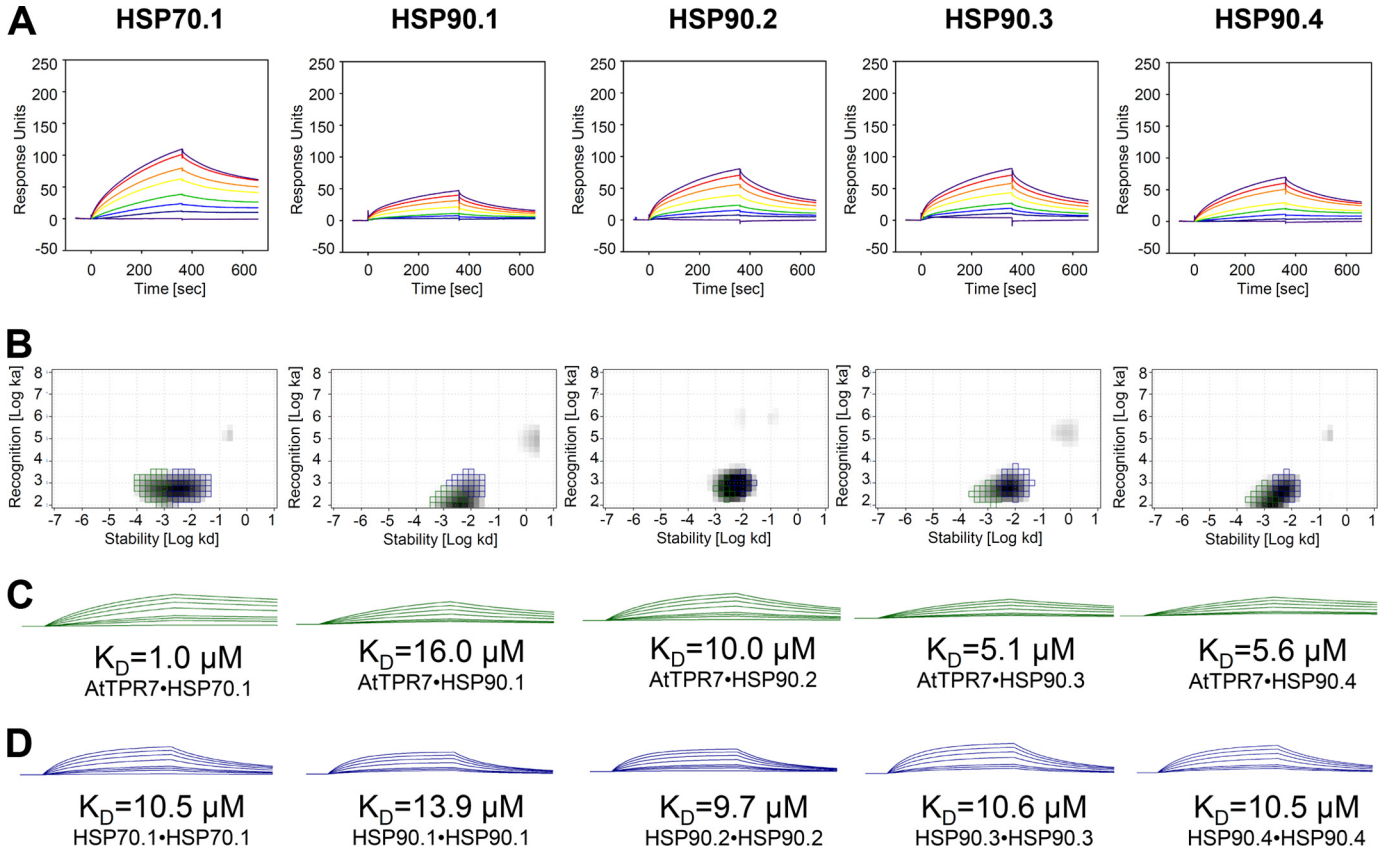

FIGURE 6. **Chaperone binding to AtTPR7 and determination of binding affinities using SPR and IM analyses.** *A,* SPR analyses. AtTPR7 was immobilized via amine coupling onto a CM5 sensor chip, and solutions of 0.1 μM (*purple*), 0.5 μM (*dark blue*), 0.75 μM (*blue*), 1 μM (*green*), 2 μM (*yellow*), 3 μM (*orange*), 4 μM (*red*), and 5 μM (*dark purple*), respectively, of each of the chaperones were passed over the chip. *B,* IM analyses. The *green spots* represent the AtTPR7-chaperone interactions and the *blue spots* the chaperone-chaperone interactions (oligomerization). *C,* calculated sensorgrams for AtTPR7-chaperone interaction. *D,* calculated sensorgrams for chaperone-chaperone interaction. The calculated K_D values for each interaction are indicated *below* the respective sensorgrams.

TABLE 1

Association (k_a), dissociation constants (k_d), and K_D values of receptor-chaperone interactions calculated by IM analysis

Chaperone	Receptor	k_a	k_d	K_D
		$1/M \cdot s$	$1/s$	μM
HSP70.1	Toc64	1.55×10^3	3.03×10^{-3}	2.0
HSP90.1		3.57×10^2	3.45×10^{-3}	9.7
HSP90.2		5.88×10^2	2.92×10^{-3}	5.0
HSP90.3		3.55×10^2	5.52×10^{-3}	15.5
HSP90.4		1.26×10^3	3.02×10^{-3}	2.4
HSP70.1	OM64	1.25×10^4	3.49×10^{-4}	0.03
HSP90.1		4.88×10^2	9.84×10^{-3}	20.2
HSP90.2		1.59×10^3	3.03×10^{-3}	1.9
HSP90.3		2.01×10^3	5.91×10^{-3}	2.9
HSP90.4		3.28×10^3	4.26×10^{-3}	1.3
HSP70.1	AtTPR7	5.41×10^2	5.25×10^{-4}	1.0
HSP90.1		1.73×10^2	2.80×10^{-3}	16.0
HSP90.2		1.72×10^2	1.73×10^{-3}	10.0
HSP90.3		3.65×10^2	1.86×10^{-3}	5.1
HSP90.4		1.97×10^2	1.10×10^{-3}	5.6

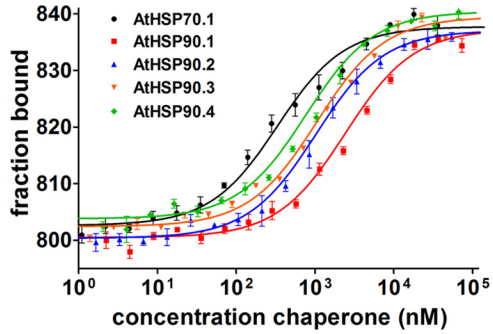

FIGURE 7. **Chaperone binding to AtTPR7 determined by MST.** Thermophoretic mobility was monitored upon chaperone titration to a constant fluorescence-labeled AtTPR7 concentration of 30 nM. Strongest binding was observed for HSP70.1 (K_D 0.3 μM) and weakest binding for HSP90.1 (K_D 2.7 μM).

TABLE 2

K_D values obtained from MST measurements with AtTPR7 and chaperones

Chaperone	Receptor	K
		μM
HSP70.1	AtTPR7	0.3
HSP90.1		2.7
HSP90.2		1.2
HSP90.3		1.2
HSP90.4		1.0

pulldown assays cannot supply quantitative data, we chose SPR combined with IM evaluation as the central method to determine binding affinities; the obtained results are summarized in Fig. 8.

Previous data on Toc64, the chloroplast-docking protein, has shown that the pea Toc64 isoform preferentially binds the C-terminal HSP90 peptide over the HSP70 peptide as determined by semi-quantitative pulldown experiments (14). We could show in our initial pulldown with the *Arabidopsis* Toc64 along with the constitutively produced full-length HSP70.1 and HSP90 isoforms that it has the potential to interact with all chaperones. SPR analyses revealed that binding affinities for all chaperones tested were in the micromolar range and showed

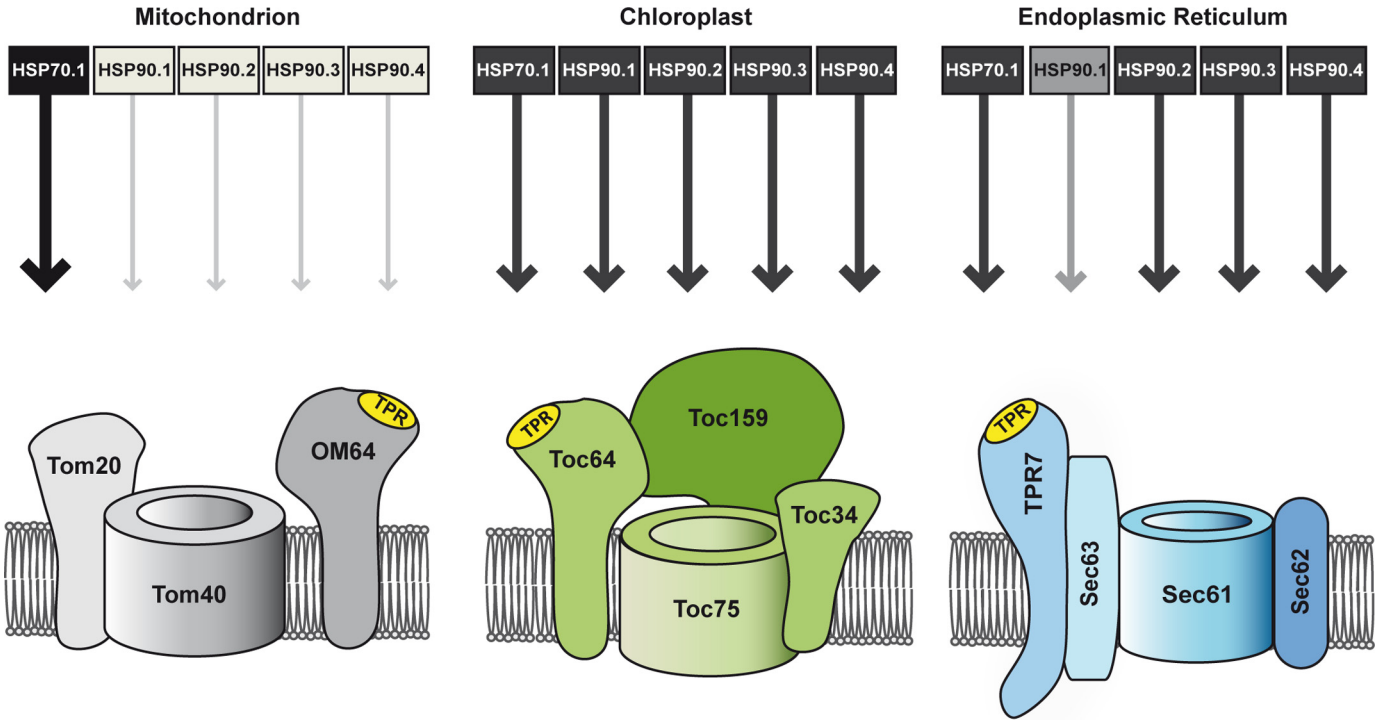

FIGURE 8. **Overview of the TPR domain-containing docking protein and chaperone binding affinities.** OM64 preferentially binds HSP70.1, whereas Toc64 associates with HSP70.1 as well as with HSP90 isoforms. AtTPR7 can interact with both HSP70.1 and HSP90 isoforms, although HSP90.1 binding is weaker. *Gray scale* and *arrow thickness* indicate binding strengths of chaperones to the respective docking proteins (*light-dark gray* corresponds to weak-strong binding).

no significant differences. However, by determining the on- and off-rates, it became evident that association constants are higher toward HSP70.1 and HSP90.4 compared with the other HSP90 isoforms, although dissociation showed comparable values for all tested chaperones. Considering that the chaperones are suggested to play a role in preprotein recognition at organellar surfaces (14), we suggest that chloroplast preproteins can be delivered with the aid of both, HSP70 and HSP90, *in vivo*. HSP90 isoforms are not discriminated and therefore are possibly functionally redundant in this context.

OM64 is phylogenetically very closely related to Toc64, showing an overall sequence identity of 51% (68% within the TPR domain) (4). However, OM64 is located in the outer mitochondrial membrane and is involved in the import of some mitochondrial preproteins (7). Therefore, it is likely that OM64 is functionally similar to the yeast and mammalian Tom70. The clamp-type TPR domain of Tom70 functions as docking site for HSP70 to receive mitochondrial preproteins, whereas mammalian Tom70 additionally binds to HSP90 (6, 12). Surprisingly, our data revealed that OM64 binds to HSP70.1 with a much higher affinity in direct comparison with the HSP90 isoforms. This tendency is evident already from the pulldown experiments, and K_D values calculated for OM64-HSP70.1 were 100 times lower, in the nanomolar range, compared with the HSP90 isoforms. In an *in vivo* situation, with HSP70 and HSP90 present in the cytosol, preferential binding of HSP70 to OM64 can be expected. Although these data are surprising, especially considering the high sequence identity between OM64 and Toc64, it favors a model in which chloroplast preproteins are assisted by HSP90, whereas mitochondrial preproteins are preferentially bound to HSP70 in the cytosol. Moreover, initial results support this hypothesis, as we have so far been unable to demonstrate HSP90 binding to plant mitochondrial preproteins, not even to hydrophobic carrier proteins,[5] mammalian counterparts of which bind to HSP90 (6).

Recently, we identified AtTPR7 as an additional TPR domain-containing docking protein associated to the ER Sec translocon in plants (19). We were interested in analyzing the binding potential to HSP90 in addition to HSP70, especially because we could detect HSP90 binding in contrast to other studies by Abell and co-workers (36, 37) (AtTPR7 is designated as OEP61 in this study). All binding affinities calculated for AtTPR7 and chaperones were found to be in the micromolar range. Although AtTPR7-HSP70.1 showed the strongest interaction, binding of AtTPR7 to HSP90 is also likely to occur *in vivo*. Interestingly, the binding affinity of HSP90.1 to AtTPR7 and OM64 was the weakest. This might indicate that the constitutively produced chaperone isoforms (HSP70.1, HSP90.2–4) play a predominant role in preprotein targeting in contrast to the mainly heat shock-induced isoform HSP90.1. Moreover, the HSP90.2, HSP90.3, and HSP90.4 isoforms are highly homologous (97–99% identity), suggesting a redundant function, whereas HSP90.1 shows only 85–87% identity to the other isoforms. The fact that we observed differences in the binding affinities of HSP90.1 to AtTPR7 and OM64 in comparison with the other HSP90 isoforms indicates that binding characteristics to the TPR domain are not only influenced by the presence of the C-terminal MEEVD motif, which is present in all HSP90 isoforms. Binding affinities seem also to be influenced by the entire protein, its

[5] S. Schwenkert, unpublished data.

FIGURE 9. **Sequence alignment of the 45 C-terminal amino acids of the four HSP90 isoforms.** *Grayscale* indicates degree of sequence similarity.

amino acid composition, as well as its higher order structure. In this respect, the C-terminal amino acids adjacent to the MEEVD motif may play a role, because they could come into close proximity to the TPR clamp of the receptor. Sequence identity in the C-terminal 45 amino acids is reduced to 73–75% when comparing HSP90.1 with the other isoforms (Fig. 9). Moreover, future structural analyses and amino acid replacements within the individual TPR domains will reveal which residues interplay with the different chaperones and participate in conferring specificity.

In addition to the SPR data set for AtTPR7, we used MST as a novel interaction analysis approach, which is surface immobilization independent. The obtained binding affinities showed the same tendency as the corresponding SPR results. Slight differences in the determined K_D values between the two methods could result from the different principles of the two techniques. Whereas in MST measurements the two proteins are allowed to interact for several minutes until the interaction has reached a steady state equilibrium, only a transient interaction is monitored by determining on- and off-rates in SPR due to the quick change between buffer and binding partner. However, clearly the same tendencies are observed, and both methods are ideally suited to act as complementary approaches.

In this study, we have used a combinatory approach of biochemical, biophysical, and computational methods to investigate protein-protein interactions and to quantify binding affinities and kinetics of three TPR receptor proteins as well as five different full-length chaperones. SPR in combination with IM and MST has proven to be a powerful approach to distinguish individual binding constants.

Acknowledgments—We thank Nano Temper (Munich, Germany), Dr. Karl Andersson (Ridgeview Instruments, Uppsala, Sweden), and Dr. Anja Drescher (GE Healthcare, Munich, Germany) for support and helpful discussions. We are grateful to Dr. Susanne Gebhard (LMU München) for critical reading of the manuscript. Katharina Schöngruber and Stefanie Rapp are acknowledged for excellent technical assistance.

REFERENCES

1. Zimmermann, R., Eyrisch, S., Ahmad, M., and Helms, V. (2011) Protein translocation across the ER membrane. *Biochim. Biophys. Acta* **1808,** 912–924
2. Schleiff, E., and Becker, T. (2011) Common ground for protein translocation: access control for mitochondria and chloroplasts. *Nat. Rev. Mol. Cell Biol.* **12,** 48–59
3. Ast, T., Cohen, G., and Schuldiner, M. (2013) A network of cytosolic factors targets SRP-independent proteins to the endoplasmic reticulum. *Cell* **152,** 1134–1145
4. Schlegel, T., Mirus, O., von Haeseler, A., and Schleiff, E. (2007) The tetratricopeptide repeats of receptors involved in protein translocation across membranes. *Mol. Biol. Evol.* **24,** 2763–2774
5. Sommer, M., Rudolf, M., Tillmann, B., Tripp, J., Sommer, M. S., and Schleiff, E. (2013) Toc33 and Toc64-III cooperate in precursor protein import into the chloroplasts of *Arabidopsis thaliana*. *Plant Cell Environ.* **36,** 970–983
6. Young, J. C., Hoogenraad, N. J., and Hartl, F. U. (2003) Molecular chaperones Hsp90 and Hsp70 deliver preproteins to the mitochondrial import receptor Tom70. *Cell* **112,** 41–50
7. Lister, R., Carrie, C., Duncan, O., Ho, L. H., Howell, K. A., Murcha, M. W., and Whelan, J. (2007) Functional definition of outer membrane proteins involved in preprotein import into mitochondria. *Plant Cell* **19,** 3739–3759
8. Scheufler, C., Brinker, A., Bourenkov, G., Pegoraro, S., Moroder, L., Bartunik, H., Hartl, F. U., and Moarefi, I. (2000) Structure of TPR domain-peptide complexes: critical elements in the assembly of the Hsp70-Hsp90 multichaperone machine. *Cell* **101,** 199–210
9. Fan, A. C., Bhangoo, M. K., and Young, J. C. (2006) Hsp90 functions in the targeting and outer membrane translocation steps of Tom70-mediated mitochondrial import. *J. Biol. Chem.* **281,** 33313–33324
10. Faou, P., and Hoogenraad, N. J. (2012) Tom34: a cytosolic cochaperone of the Hsp90/Hsp70 protein complex involved in mitochondrial protein import. *Biochim. Biophys. Acta* **1823,** 348–357
11. Bhangoo, M. K., Tzankov, S., Fan, A. C., Dejgaard, K., Thomas, D. Y., and Young, J. C. (2007) Multiple 40-kDa heat-shock protein chaperones function in Tom70-dependent mitochondrial import. *Mol. Biol. Cell* **18,** 3414–3428
12. Chan, N. C., Likić, V. A., Waller, R. F., Mulhern, T. D., and Lithgow, T. (2006) The C-terminal TPR domain of Tom70 defines a family of mitochondrial protein import receptors found only in animals and fungi. *J. Mol. Biol.* **358,** 1010–1022
13. Feldheim, D., and Schekman, R. (1994) Sec72p contributes to the selective recognition of signal peptides by the secretory polypeptide translocation complex. *J. Cell Biol.* **126,** 935–943
14. Qbadou, S., Becker, T., Mirus, O., Tews, I., Soll, J., and Schleiff, E. (2006) The molecular chaperone Hsp90 delivers precursor proteins to the chloroplast import receptor Toc64. *EMBO J.* **25,** 1836–1847
15. Qbadou, S., Becker, T., Bionda, T., Reger, K., Ruprecht, M., Soll, J., and Schleiff, E. (2007) Toc64–a preprotein-receptor at the outer membrane with bipartide function. *J. Mol. Biol.* **367,** 1330–1346
16. Sohrt, K., and Soll, J. (2000) Toc64, a new component of the protein translocon of chloroplasts. *J. Cell Biol.* **148,** 1213–1221
17. Carrie, C., Murcha, M. W., and Whelan, J. (2010) An *in silico* analysis of the mitochondrial protein import apparatus of plants. *BMC Plant Biol.* **10,** 249
18. Chew, O., Lister, R., Qbadou, S., Heazlewood, J. L., Soll, J., Schleiff, E., Millar, A. H., and Whelan, J. (2004) A plant outer mitochondrial membrane protein with high amino acid sequence identity to a chloroplast protein import receptor. *FEBS Lett.* **557,** 109–114
19. Schweiger, R., Müller, N. C., Schmitt, M. J., Soll, J., and Schwenkert, S. (2012) AtTPR7 is a chaperone-docking protein of the Sec translocon in *Arabidopsis*. *J. Cell Sci.* **125,** 5196–5207
20. Schweiger, R., and Schwenkert, S. (2013) AtTPR7 as part of the Arabidopsis Sec post-translocon. *Plant Signal. Behav.* **8,** doi 10.4161/psb.25286
21. Sung, D. Y., Vierling, E., and Guy, C. L. (2001) Comprehensive expression profile analysis of the *Arabidopsis* Hsp70 gene family. *Plant Physiol.* **126,** 789–800
22. Krishna, P., and Gloor, G. (2001) The Hsp90 family of proteins in *Arabidopsis thaliana*. *Cell Stress Chaperones* **6,** 238–246
23. Schmid, A. B., Lagleder, S., Gräwert, M. A., Rähl, A., Hagn, F., Wandinger, S. K., Cox, M. B., Demmer, O., Richter, K., Groll, M., Kessler, H., and Buchner, J. (2012) The architecture of functional modules in the Hsp90 co-chaperone Sti1/Hop. *EMBO J.* **31,** 1506–1517
24. Lamberti, G., Gügel, I. L., Meurer, J., Soll, J., and Schwenkert, S. (2011) The cytosolic kinases STY8, STY17, and STY46 are involved in chloroplast differentiation in *Arabidopsis*. *Plant Physiol.* **157,** 70–85
25. Fellerer, C., Schweiger, R., Schöngruber, K., Soll, J., and Schwenkert, S. (2011) Cytosolic HSP90 cochaperones HOP and FKBP interact with freshly synthesized chloroplast preproteins of *Arabidopsis*. *Mol. Plant* **4,** 1133–1145
26. Zhang, X. P., and Glaser, E. (2002) Interaction of plant mitochondrial and

chloroplast signal peptides with the Hsp70 molecular chaperone. *Trends Plant Sci.* **7,** 14–21
27. Thompson, A. D., Bernard, S. M., Skiniotis, G., and Gestwicki, J. E. (2012) Visualization and functional analysis of the oligomeric states of *Escherichia coli* heat shock protein 70 (Hsp70/DnaK). *Cell Stress Chaperones* **17,** 313–327
28. Kadota, Y., and Shirasu, K. (2012) The HSP90 complex of plants. *Biochim. Biophys. Acta* **1823,** 689–697
29. Nemoto, T., and Sato, N. (1998) Oligomeric forms of the 90-kDa heat shock protein. *Biochem. J.* **330,** 989–995
30. Aprile, F. A., Dhulesia, A., Stengel, F., Roodveldt, C., Benesch, J. L., Tortora, P., Robinson, C. V., Salvatella, X., Dobson, C. M., and Cremades, N. (2013) Hsp70 oligomerization is mediated by an interaction between the interdomain linker and the substrate-binding domain. *PLoS One* **8,** e67961
31. Barta, P., Björkelund, H., and Andersson, K. (2011) Circumventing the requirement of binding saturation for receptor quantification using interaction kinetic extrapolation. *Nucl. Med. Commun.* **32,** 863–867
32. Altschuh, D., Björkelund, H., Strandgård, J., Choulier, L., Malmqvist, M., and Andersson, K. (2012) Deciphering complex protein interaction kinetics using Interaction Map. *Biochem. Biophys. Res. Commun.* **428,** 74–79
33. Seidel, S. A., Dijkman, P. M., Lea, W. A., van den Bogaart, G., Jerabek-Willemsen, M., Lazic, A., Joseph, J. S., Srinivasan, P., Baaske, P., Simeonov, A., Katritch, I., Melo, F. A., Ladbury, J. E., Schreiber, G., Watts, A., Braun, D., and Duhr, S. (2013) Microscale thermophoresis quantifies biomolecular interactions under previously challenging conditions. *Methods* **59,** 301–315
34. Carrigan, P. E., Nelson, G. M., Roberts, P. J., Stoffer, J., Riggs, D. L., and Smith, D. F. (2004) Multiple domains of the co-chaperone Hop are important for Hsp70 binding. *J. Biol. Chem.* **279,** 16185–16193
35. Brinker, A., Scheufler, C., Von Der Mulbe, F., Fleckenstein, B., Herrmann, C., Jung, G., Moarefi, I., and Hartl, F. U. (2002) Ligand discrimination by TPR domains. Relevance and selectivity of EEVD-recognition in Hsp70·Hop·Hsp90 complexes. *J. Biol. Chem.* **277,** 19265–19275
36. Kriechbaumer, V., Tsargorodskaya, A., Mustafa, M. K., Vinogradova, T., Lacey, J., Smith, D. P., Abell, B. M., and Nabok, A. (2011) Study of receptor-chaperone interactions using the optical technique of spectroscopic ellipsometry. *Biophys. J.* **101,** 504–511
37. von Loeffelholz, O., Kriechbaumer, V., Ewan, R. A., Jonczyk, R., Lehmann, S., Young, J. C., and Abell, B. M. (2011) OEP61 is a chaperone receptor at the plastid outer envelope. *Biochem. J.* **438,** 143–153